Accepted Manuscript

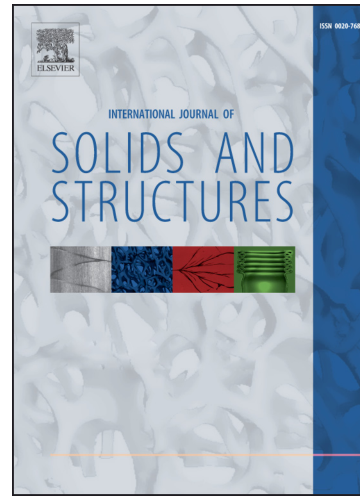

Failure theory via the concept of material configurational forces associated with the *M*-integral

NingYu Yu, Qun Li

PII: S0020-7683(13)00348-X
DOI: http://dx.doi.org/10.1016/j.ijsolstr.2013.09.001
Reference: SAS 8106

To appear in: *International Journal of Solids and Structures*

Received Date: 15 March 2013
Revised Date: 15 August 2013

Failure theory via the concept of material configurational forces associated with the *M*-integral

NingYu Yu, Qun Li*

State Key Laboratory for Strength and Vibration of Mechanical Structures, School of Aerospace, Xi'an Jiaotong University, 710049, P.R. China

*Correspondence author (Tel: ++86-29-82668754; E-mail: qunli@mail.xjtu.edu.cn)

Abstract

A new failure theory based on the material configuration forces associated with the invariant *M*-integral is proposed to describe the content and evolution of the multi-defects localized in the body. The physical interpretation of the global *M*-integral is explored as the sum of the local energy release rate due to the self-similar expansion for each specific defect. It does provide an effective measure for the evaluation of damage level. It is found that the unique parameter of the *M*-integral cannot be used as a unified failure criterion to predict the damage evolution and the final failure due to the major obstacle that the critical value of the *M*-integral is not a problem-invariant constant and shows an apparent defect configuration-dependence. Consequently, a new failure parameter referred as the Configurational Damage Parameter (abbreviated as -parameter) is proposed by the appropriate formulation via the *M*-integral, the remote uni-axial load, and the inner variable of the damaged area. A series of numerical examples are carried out to demonstrate that the critical value of -parameter is a material constant regardless of defect configurations. Furthermore, it is performed to validate the applicability of the -parameter as a failure criterion to predict the final failure of the locally damaged materials. Finally, a protocol of experimental measurement of the -parameter is proposed by method of digital image correlation to facilitate the wide application of the new failure criterion. It is concluded that the present failure theory via the configurational forces associated with the *M*-integral provides some outside variable features and has the advantage of predicting the structural integrity of damaged materials containing the locally distributed defects.

Keywords: Failure theory; J_k-integral; *M*-integral; *L*-integral; Material configurational force; Configurational damage parameter

1. Introduction

The lifetime, strength, and integrity of structural components are substantially limited by the existence of microdefects such as microcracks, microvoids, micro-inclusions, or dislocations. The severe inhomogeneity caused by such defects may induce damage evolution, macroscopic crack, and even final failure. In order to predict the failure of materials, there are several failure criterions proposed by many researchers in past decades. The pioneering one is the linear elastic theory of strength. That is, the body is supposed to fracture when the maximum stress $_{max}$ in the body reaches the strength of material $_{b}$ (Ford, 1963; Kanninen and Popelar, 1985). For the ductile material with defects, the classical strength theories, e.g., the maximum principle stress theory $_{max}$ $_{b}$, are still widely used in both mechanical and civil engineering. However, the linear elastic theory of strength is hard to use in practice since the maximum stress in a body is sensitive to the shape of defects and the procedure assumes that the strength of a material is independent of the sample used in the experiment. In reality, material strengths measured from different samples are diverse due to the various configurations of intrinsic defects.

The real materials are generally assumed to contain a multitude of defects uniformly distributed in the body in the initial state. The internal defects may grow and coalesce by the creation of new microdefects at stress concentrators. This will cause a change of the macroscopic material properties and the decrease of strength. It leads to a complete failure of material's integrity and the formation of a macroscopic crack. Within the framework of damage mechanics, the state (extent) of damage is represented by a so-called damage variable, such as the damage volume fraction f (internal variable) or the effective elastic moduli E (outside variable). They are used to characterize geometric quantification of brittle and ductile damage, respectively. Macroscopic strains and stresses are represented by the volumetric averages over the whole representative volume. Such damage model is able to describe the material failure behaviors during the process of deformation until total loss of the stiffness. The final failure could be described by the critical value of damage variables f=f_c, or the effective elastic moduli E=E_c for instance (Kachanov, 1986).

In the course of a deformation process, the growth and coalescence of internal microdefects leads to the formation of a macroscopic crack. The linear elastic fracture mechanics is emerged based on the concept of stress intensity factors and energy release rate. The stress field is quantified by the stress intensity factor, or K-factor for short (Irwin, 1957). The fracture criterion based on the K-factor is formulated as the crack propagation starts when the K-factor reaches the material-specific critical value K_C. Base on the viewpoint of energy balance, the concept of energy release rate is proposed by Griffith (1921). The material specific value called G criterion, or crack resistance, is proposed to predict the crack stability. In the framework of linear elastic fracture mechanics, the failure criterions of K=K_C and G=G_C are equivalent for the pure crack mode in linear elasticity.

For elastic-plastic materials containing one or more macroscopic cracks, the crack tip fields have to be determined by considering the plastic behaviors near the crack tips. The stress intensity factors and the energy release rate determined by the crack tip fields have to be adopted with cautions under the large scale yielding assumption. The so-called invariant integrals such as the J-integral have been widely applied in fracture mechanics to determine the crack tip parameters. The intensity factors and the energy release rate can be represented in terms of field variables by the J-integral calculated along the remote contours away from the plastic zone near the crack tips. Furthermore, by replacing the intensity factors and the energy release rate, the J-integral can be used as an effective fracture parameter to predict the crack stability and growth in elastic-plastic materials. It is well known that the ductile fracture could be governed by J J_{IC}, i.e., the so-called J-dominant criterion (Cherepanov, 1967; Rice, 1968).

Actually, the introduction of the J-integral is referred to the mechanics in material space in contrast with Cauchy stress in Newtonian space. The other series of well-known invariant integrals derived from Neother's theorem in plane elasticity include the J_1 (J)-, J_2-, M-, and L-integral (Knowles and sterberg, 1972; Budiansky and Rice, 1973; Eshelby, 1975; Freund, 1978). These invariant integrals can be obtained by the corresponding material configurational forces which are obtained by the gradient, divergence, and curl operation of the Lagrangian function, respectively. For instance, deduced from the gradient of Lagrangian function, the configuration forces associated with the J_k-integral can be derived, which is well-known as the Eshelby tensor. The invariant integrals including the J_k-, M-, and L-integral are widely researched in previous literatures (see the reviews by Chen, 2002; Chen and Lu, 2003). However, the latter two integrals, the M-integral and the L-integral, received much less attention than the J-integral does. The available applications of both the M-integral and L-integral are limited for problems with a single crack (Herrmann and Herrmann, 1981; Chen, 1986; Eischen and Herrmann, 1987; Choi and Earmme, 1992; Seed, 1997; Chen, 2003; Chen and Lee, 2004). They did provide some numerical techniques to determine the crack tip parameters. For example, Lee and Im (2003) examined the stress intensities of the three-dimensional wedges, and proposed a general scheme to compute the singular stress states near the vertices using two-state M-integral. However, the M-integral and L-integral were rarely used to give some engineering applications to estimate the failure or the life of engineering components. The successful application of the J-dominant criterion in fracture mechanics really puts the M-integral and the L-integral in the shade in past decades.

The main purpose of this paper is to propose a new failure theory via the concept of configurational forces associated with the invariant integrals. The innovative idea is originated from two aspects of considerations. On one hand, if one estimates the stability or integrity of materials containing the locally distributed defects as shown in Fig. 1(a), where there are neither major macroscopic cracks nor the uniformly distributed defects, the traditional failure theories will be challenged to determine the critical failure load and predict the structural integrity. For example, the classic fracture mechanics based on the stress intensity factors, the energy release rate, or the J-integral near the crack tips is hard to use in practice since they require one or more macroscopic cracks with the measured length and configuration. It is obviously a challenge to distinguish the specific crack tips in the multi-damaged material in Fig. 1(a). The classic damage mechanics relying on the inner variables requires the uniformly distributed defects in materials, which is not suitable for the present locally damaged materials either. On the other hand, the damage procedure can be demonstrated by the total energy release rate due to the configurational evolution of defects. Indeed, the J_k-, M-, and L-integral have the apparent physical interpretations and they can be explained as the energy release rates due to the translation of defects along x_k-direction, the self-similar expansion, the rotation of defects, respectively. When the contour enclosing all defects is selected to calculate the invariant integrals, as depicted in Fig. 1(b), the energy release rate can be totally represented by the calculated invariant integrals. Such a flexibility physical interpretation of invariant integrals implies that they have potential applicability to predict the failure of multi-defect materials and structures. It is encouraged to provide an appropriate failure theory via the concept of the configurational forces associated with these invariant integrals.

It should be pointed that the direct application of the J_k-integral in fracture mechanics to the multi-defect materials will be limited by the well-known conservation laws of the J_k-integral concluded by Chen and Hasebe (1998). That is, both two components of the J_k vector vanish under remote uniform loads when the closed contour completely encloses all the defects. It means that the J_k-integral make little effort to construct the failure parameter via the invariant integrals for such multi-defect problems. Consequently, the M-integral and the L-integral would play the key role instead of the J_k-integral. Recently, Chen (2001a, 2001b) proposed an M-integral description to study a cloud of microcracks in an infinite plane brittle solid. Instead of working in the continuum damage mechanics, his investigation started from the Eshelby's energy momentum tensor and the associate invariant integrals. Particularly, it is concluded that the M-integral is inherently related to the change of the total potential energy for a 2D linear damaged elasticity regardless of the detailed damage characterizations. Following Chen's work, the M-integral analysis was performed by Chang and Chien (2002), Chang and Peng (2004), Chang and Wu (2011). A problem-invariant parameter in those works was defined by performing the M-integral with respect to a coordinate system originating at the geometric center of all the singular points enclosed by the integration contour. The distinguished work by Chang et al (2002, 2004 and 2011) is greatly appreciated. They also suggest that M-integral might be proposed as a possible damage parameter for describing the degradation of material and structural integrity caused by the irreversible evolution of multiple defects. They considered the formulation to be suited for fracture analysis in rubbery material problems which subject to large elastic deformation.

More recently, Hu and Chen (2009a, 2009b) performed some finite element analyses for a plane strip containing two neighborly located voids or cracks, and demonstrated the change of M-integral before and after the coalescence of the defects. It is concluded that there is a jump of the M-integral when the coalescence of the two cracks or voids occurs and the M-integral can be used to describe the damage evolution. In addition, Wang and Chen (2010) proposed a new parameter $d(M+L)/dN$ based on the M-integral and L-integral concepts to solve the fatigue damage problem of an Aluminum plane strip with neighborly and symmetrically located voids under cyclic tensile loading. The technique proposed by the previous work demonstrates that the invariant integrals did play an important role in the description of the multi-damage problems. Following this conclusion, a number of subsequent analysis of invariant integrals in nano-mechanics were applied to measure the damage levels of nano-porous membrane in which the surface effects were taken into account(e.g., Li and Chen, 2008; Hui and Chen, 2010; Hu et al, 2012). All studies demonstrate that the configurational forces associated with the *M*-integral emerge as a failure criterion which is capable of describing the damage behavior of a multi-damaged mechanical system similar as what the *J*-integral does in fracture mechanics. It can provide some outside variable features which might introduce a new technique or framework to evaluate material damage evolution.

The present work is to address a new failure theory for the multi-defects system, especially the locally damaged solid. The framework of the new failure theory is referred to the apparent physical interpretation of the invariant integrals. The total energy release involving the microdefects cloud translation, expansion, and rotation can be represented by the J_k-, *M*-, and *L*-integral, respectively. A series of multi-defects examples are considered. The inherent relation between the *M*-integral and the reduction of effective elastic moduli is studied by both numerical and theoretical analysis. The critical values of the *M*-integral (M_C) and *L*-integral (L_C) are numerically evaluated. It is found that the *L*-integral has the negligible contribution compared with the remarkable *M*-integral does. Therefore, we pay more attention to the *M*-integral in describing damage evolution. In order to clarify whether M_C is a critical problem-invariant constant for the materials with multiple voids or cracks, the possible dependence of M_C on the multi-defect configurations is carried out. It is found that the critical value of the *M*-integral is not a material-specific constant. Instead of the directly applying the *M*-integral as the failure criterion, the new failure theory via the Configurational Damage Parameter (-parameter) is established, which is determined by both inner and outside variables of the damaged materials such as the *M*-integral, the external load, and the damaged area. The present analysis illustrated in a number of numerical examples demonstrates that the proposed failure theory is effective and convenient for the locally damaged materials. To this end, an efficient protocol to experimentally measure the configurational damage parameter is introduced by method of digital image correlation.

2. Material configurational forces associated with the J_k-, M-, and L-integral

The derivative of material configurational forces can be generally referred to Noether's first theorem for a multi-defects system. It turns out to be an effective way to explicitly define the invariant integrals formulated by the corresponding material configurational forces. The present methodology for establishing material configurational forces associated with the J_k-, M-, and L-integral is based on the Lagrangian energy density.

In the absence of inertia terms and body force, the Lagrangian function Λ may be looked upon as a potential. It can be identified as the negative of the strain energy density of system which depends, in general, on the independent variable of coordinates and the first derivatives of displacement i.e.,

$$\Lambda(x_i, u_{k,j}) = -W(x_i, u_{k,j}). \tag{1}$$

The fundamental concepts of material configurational forces regarding the J_k-, M-, and L-integrals are reviewed and summarized in Table 1 for the convenience of readers. The detailed descriptions can refer to the references (Knowles and Sternberg, 1972; Eshelby, 1975; Chen and Shield, 1977; Kienzler and Herrman, 1997; Lee and Im, 2003; Li et al, 2012 among many others).

In order to clarify the physical interpretation of the configurational forces M_j associated with the M-integral, a self-similar expansion of the element with the unit thickness is studied such that points (x_1, x_2) on the surfaces move with the distance of (x_1dt, x_2dt). Fig. 2(a, b) depicts the transformation from the original element indicated by the solid black square into the expanded element by the dash square along the x_1- and x_2-direction, respectively. The physical interpretation of the configurational forces regarding the M-integral can be deduced by the potential energy change during the self-similar expansion motion of element. That is, the component of M_j is the change of the potential energy at a point of an elastic continuum due to a self-similar expansion in x_j-direction of a unit surface. A straightforward physical interpretation of the M-integral for a multi-damage system can be made based on the present physical meaning of configuration forces. The M-integral is associated with the integration of the configuration force M_j along a close contour. If we calculate the M-integral over the specific contour C_s (s=1, 2, ….., N) surrounding only the s-th defect, as shown in Fig. 2(c), the local M-integral for the specific s-th defect over C_s and the global M-integral for all defects over Γ can be expressed as:

$$
\begin{aligned}
M^{(s)} &= \oint_{C_s} (w x_i n_i - T_k u_{k,i} x_i) ds; \\
M &= \sum_{s=1}^{N} M^{(s)} = \oint_{\Gamma} (w x_i n_i - T_k u_{k,i} x_i) ds;
\end{aligned} \tag{2}
$$

The physical interpretation of local $M^{(s)}$ can be given as the energy release due to the self-similar expansion for the specific s-th defect. Therefore, the global M-integral over the contour Γ enclosing all defect can be interpreted as the sum of local energy release due to the self-similar expansion for each specific defect.

Similarly, the physical interpretation of the configurational forces b_{ji} (i, j=1, 2) can be explained as the change of the total energy density at a point of an elastic continuum due to a material unit translation in x_j-direction of a unit surface with normal in x_i–direction (Kienzler and Herrmann, 1997). The physical interpretation of local $J_k^{(s)}$-integral over the specific contour C_s (s=1, 2, ….., N) only surrounding the s-th defect can be given as the energy release due to the translation $x_{k0}^{(s)}$ along x_k-direction for the specific s-th defect. And the global J_k-integral over the contour Γ enclosing all defect is interpreted as the sum of local energy release due to the translation of defects along x_k-direction.

The physical meaning of the configurations forces L_{ml} will be related to the change of the potential energy of the element associated with the specific rotation motion. Assume that a rotational movement of the infinitesimal element is under consideration with respect to the reference point. After rotation, an ordinary point (x_1, x_2) in the element has the displacements along both horizontal and vertical direction. The point (x_1, x_2) on the element surface is moving with the following velocity v_i=-$e_{3ij}x_j\omega$ (i, j=1, 2), where is a positive constant and represents the angular velocity with respect to the specific point. The real physical interpretation of the component L_{3i} of the configurational forces is indentified as the change of potential energy of one infinitesimal element on the surface with normal direction along x_i if the material element has the rotation motion with respect to the reference point. The physical interpretation of local $L^{(s)}$-integral is given as the energy release due to the rotation $_0^{(s)}$ for the specific s-th defect. And the global L-integral is interpreted as the sum of energy release due to the rotation for each specific defect.

3. The proposed failure criterion

3.1 Numerical examples

In order to propose the failure criterion via the concept of material configurational forces, finite element analyses are performed to consider the multiple microdefects in materials. It should be emphasized that the J_k-integral enclosing all defects satisfies the conservational laws and would vanish during damage evolution. Consequently, only the *M*-integral and *L*-integral will be calculated without further consideration of the J_k-integral. A series of numerical examples are carried out to provide necessary evidences of the role which the material configurational forces associated with the *M*-integral and *L*-integral plays in predicting the failure of multi-damaged materials.

Fig. 3 shows the configuration of the damaged zone locally located at the center of an elastic plate. The damaged zone is distributed with multiple defects, including microvoids or microcracks. The dimensions of the inner damaged zone are 12mm 12mm (length width) while the full dimensions of the plate are 160mm 40mm (length width) with w_1, w_2, l_1, l_2 being the width, length of the plate and the damaged zone as indicated in Fig. 3. The elastic plate is made of Aluminum alloy LY-12 with the Young's elastic modulus E=71 GPa and the Poisson's ratio =0.33 while the damaged zone localized in the body is assumed to shows a typical nonlinear curve of stress-strain relation (see Fig. 4) with a typical power hardening feature.

In this paper, two different defect patterns are considered. One defect pattern is concerned with the microvoids which are locally distributed in the inner damaged zone. Each void has the same diameter of 0.5*mm*. Various numbers of microvoids are taken into account to represent the various defect densities, i.e., 9, 16, 25, 36, 49, 64, 81, 100, 121, 144, 169 voids as depicted in Fig. 5. The other pattern is filled with microcracks which are locally distributed in both position and relative orientation. Each crack has the length of 0.5*mm*. Various numbers of microcracks are also considered, i.e., 9, 16, 25, 36, 49, 64, 81, 100, 121, 144, 169 cracks as depicted in Fig. 6. Each defect pattern with the specific number of defects represents one specific defect configuration. It means there are totally 22 defect configurations concerned in numerical analyses.

It is emphasized that the path-independence of the *M*-integral and *L*-integral should be re-clarified in nonlinear elastic-plastic materials. An explicit analysis of the invariant integrals in the nonlinear solid reveals that the material inhomogeneity induced by defects together with the nonlinear strain energy within the area enclosed by the integration contours will be dominant contributions on the invariant integrals. The influence of the nonlinear strain energy will result in the path-dependence property of the invariant integrals (e.g., McMeeking, 1977; Kuang and Chen, 1996; Carka and Landis, 2011; Li et al, 2012). This is quite different from that of linear elasticity where the invariant integrals are always path-independent. In order to avoid the unexpected path-independent issues, the present study assumes that the nonlinear deformation is localized inside the damaged zone located at the center of the plate while the outer region is assumed to be linear elasticity. Therefore, the *M*-integral and *L*-integral are calculated along the contour in the elastic zone far away from the damaged plastic zone. A rectangle contour shown in Fig. 3 is selected in the remote elastic zone completely surrounding the elastic-plastic damaged zone.

3.2 Numerical results of the M-integral and the reduction of effective elastic moduli

In this section, attention is focused on the tendency of the *M*-integral and the effective elastic moduli for the increasing external loading. The relation between the values of the *M*-integral and the classical strength theory defined by the reduction of effective elastic moduli is addressed in multi-damaged material. This finding will facilitate the introduction of the proposed failure theory for the purpose of the present study.

First, Fig. 7 shows the calculated values of the *M*-integral against the uni-axial remote loadings for the locally distributed microvoids, while Fig. 8 for the locally distributed microcracks. It can be seen from Figs. 7 and 8 that the *M*-integral monotonically increases with the increasing loading. Additionally, the values of the *M*-integral are strongly sensitive to the numbers of the defects. The more the defects exist, the larger value of the *M*-integral is. Particularly, for the defect-free material in which there is no defect inside the damaged zone, the values of *M*-integral in Figs. 7 and 8 are still remarkable. The present study considers that the plastic deformation is under a single load parameter in the absence of elastic unloading. Therefore, the plastic deformation is approximately represented by the nonlinear elastic deformation. The opinion is accepted that when a body is subject to proportional loading, the stress-strain behavior of plastic deformation is indistinguishable from that of nonlinear elastic deformation. It is denoted that the nonlinear elastic energy enclosed by the integral contours will have a significant contribution on the values of the *M*-integral. A consistent conclusion can be analytically made regarding the contribution of the nonlinear elastic energy to the *M*-integral (see Appendix A) for the defect-free medium. In is denoted that the *M*-integral not only represents the discontinuities induced by the defects, but also describes the emergence of nonlinear elastic energy with the increasing loading. The remarkable role of the *M*-integral can be concluded that it can provide some important evidences of microstructural statistical information. The physical characterization actually embedded in the formulation of the phenomenological parameter of the *M*-integral could be a useful concept to describe the degradation of structural integrity, which is caused by irreversible evolution of multiple microvoids or cracks.

Second, numerical determination of the effective properties of multi-defect system is performed by involving the calculation of the stress and strain fields averaged over the representative volume element (Banerjee and Adams, 2004). The effective elastic stiffness tensor C_{ijkl}^{eff} is calculated from the material constitutive relation

$$\int_V \sigma_{ij} dV = C_{ijkl}^{eff} \int_V \varepsilon_{kl} dV, \tag{3}$$

where σ_{ij} and ε_{kl} are the local stress and strain tensor and V is the representative volume element. For the plane stress condition in this research, the formulation could be simply written as

$$\begin{bmatrix} \langle \varepsilon_{11} \rangle_V \\ \langle \varepsilon_{22} \rangle_V \\ \langle \varepsilon_{12} \rangle_V \end{bmatrix} = \begin{bmatrix} 1/E_{11}^{eff} & -\nu_{21}^{eff}/E_{11}^{eff} & 0 \\ -\nu_{12}^{eff}/E_{22}^{eff} & 1/E_{22}^{eff} & 0 \\ 0 & 0 & 1/G_{12}^{eff} \end{bmatrix} \begin{bmatrix} \langle \sigma_{11} \rangle_V \\ \langle \sigma_{22} \rangle_V \\ \langle \sigma_{12} \rangle_V \end{bmatrix}, \tag{4}$$

where E_{11}^{eff}, E_{22}^{eff}, ν_{12}^{eff}, and ν_{21}^{eff} are two-dimensional Young's elastic moduli and Poisson's ratios, and $\langle \varepsilon_{ij} \rangle_V$ and $\langle \sigma_{kl} \rangle_V$ are the average of strain and stress tensors over the representative volume. In the present numerical calculations, the local damaged zone inside the plate is considered as the representative volume to calculate the effective elastic moduli instead of the whole plate.

Fig. 9 and Fig. 10 plot the vertical effective elastic moduli against the remote loading for the locally distributed microvoids or microcracks. It can be seen that there is an apparent reduction of effective moduli with the increasing loading compared with E=71 GPa of LY-12 matrix. The tendency of the effective elastic moduli against the tensile loading can be demonstrated as two variable tendencies. One is that the magnitude of the effective elastic moduli shows a constant value lower than the elastic moduli of LY-12 matrix for all defect cases when the tensile loading is lower than the yielding stress of elastic-plastic materials. The reduction of effective elastic moduli mainly results from the existence of the microvoids or microcracks, which alleviate the material strength. At this stage, the elastic-plastic material behavior has little influence on the reduction of effective elastic moduli. The other tendency of the effective elastic moduli shows a sharp decrease when the external loading reaches a certain magnitude. This strong reduction of moduli results from the elastic-plastic material behaviors. When the stress reaches the yielding stress of material, the material behavior has a transformation from linear elastic to nonlinear plastic state. The effective elastic moduli have a consequent transformation from the constant to a sharp reduction.

Of the most importance is that there exists an implicit relation between the *M*-integral and the reduction of effective moduli for the multi-damaged solids. The reduction of effective elastic moduli just shows an apparent positive feature to those of the *M*-integral. Indeed, the maximum values of the *M*-integral occur at the maximum tensile load, whereas the maximum values of the reduction of effective moduli corresponding to the least effective modulus at the maximum tensile load. The inherent relation between the *M*-integral and the reduction of effective elastic moduli can be concluded for the multi-damaged problem. That is, the larger value of the *M*-integral under the certain loading is, the larger reduction of effective elastic moduli reduced from the microdefecting or elastic-plastic material behaviors is.

Numerical results do provide necessary evidences of the implicit relation between the *M*-integral and the reduction of effective elastic moduli in the locally distributed damage problems. In order to further demonstrate this inherent relation, an explicit analysis of the infinite elastic matrix with the elastic moduli E containing a circular inhomogeneity with the reduced elastic moduli E_0=(1-)E is performed by the classic complex potential theory, where denotes the reduction of the elastic moduli of inhomogeneity versus the matrix. The analytical expression of the *M*-integral for the infinite elastic matrix embedded a circular inhomogeneity with the reduced moduli can be obtained as (see Appendix B)

$$M=\frac{\pi\sigma^2R^2(1-\nu^2)}{E}f(\alpha) \tag{5}$$

where *f*( ) is the explicit function of elastic moduli reduction   formulated by

$$f(\alpha)=\frac{(-3\nu^2-5)\alpha^2+(6\nu^2-6\nu\nu_0+8)\alpha+(-3\nu^2-3\nu_0^2+6\nu\nu_0)}{(-\nu^2+2\nu+3)\alpha^2+(2\nu^2-2\nu\nu_0+2\nu_0-4\nu-10)\alpha+(-\nu^2+2\nu\nu_0+2\nu-\nu_0^2-2\nu_0+8)}$$

Eq.(5) reveals that the *M*-integral is inherently related with the reduction of Young's moduli of inhomogeneity. Fig. 11 shows the *M*-integral against   according to Eq.(5) assuming that inhomogeneity has the same Poisson's ratio as the matrix, i.e., = $_0$=0.33. It is seen that the *M*-integral is monotonically increased with the increase of the reduction of elastic moduli. This explicit analysis is consistent with the present numerical results. It should be pointed that the present numerical examples are carried out for the locally multi-damaged square zone embedding in the finite plate whereas the theoretical analysis is particularly introduced for the circular inhomogeneity in the infinite elastic plane. The numerical examples are slightly different from the appended theoretical problem. Nevertheless, if we assume the multi-damaged zone as a specific inhomogeneity, the present explicit investigation can be an approximate evidence to verify the inherent relation between the *M*-integral and the reduction of effective elastic moduli of the multi-damaged zone.

3.3 Critical values of the M-integral and the L-integral

The successful application of the *J*-dominant criterion used in fracture mechanics attributes to the critical value of J_C, which is a material-specific constant regardless the crack size and configurations. Similar as the *J*-integral, a forward and straight idea emerges whether the direct application of the *M*-integral or the *L*-integral is able to be promoted where one might introduce a problem-invariant parameter M_C or L_C (the critical value of the *M*-integral or the *L*-integral when the failure happens). The key issue of the introduction of the *M*-integral or the *L*-integral as a failure criterion is to clarify the features of M_C or L_C. Numerical investigations are carried out to verify whether M_C or L_C is the critical problem-invariant constant for the multi-damaged material. In order to confirm the critical loading for multi-damaged materials, the classic strength theory that the reduction of elastic moduli reaches the critical values is under consideration as an alternative way. For this purpose, the critical values of the *M*-integral and the *L*-integral are defined as the reduction of effective elastic moduli reaches a criterion values e.g., 0.47 for the present LY-12 alloy.

Fig. 12 and Fig. 13 show the critical values of the M-integral and L-integral for the locally distributed microvoids or the microcracks problems. It is found that the critical values of the M-integral is always positive and represents the energy release due to self-similar expansion of multi-defects while the L-integral could be either positive or negative depending on the specific configuration microvoids or cracks. The magnitude of negative L-integral represents the energy absorbing due to the rotation of microdefects. Furthermore, it is found that the magnitudes of the critical L-integral are negligible comparing with those of the M-integral. It implied that the L-integral has little effort to control the damage evolution in present examples. Beside the conservation laws of the J_k-integral where the values of J_k-integral is always zero as long as the integral contour enclosing the multi-defects, only the M-integral among three well-known invariants (J_k-, M-, and L-integral) has the major effort to control the failure of multi-damaged materials. Consequently, special attention will be focused on the M-integral in the sequent discussions.

It is found that the critical M-integral does apparently depend on the defect density and defect pattern. Numerical responses of M_C corresponding to different number of multi-defects and the critical tensile loading for evolution of multi-defects show that the critical value of the M-integral and the extern load appears to monotonically decrease with the increasing number of multi-defects. That is, the less the number of defects is, the larger critical values of the M-integral and the critical loading are. For instance, the minimum value of M_C is approximately 26 N with respect to 169 voids under the critical loading 142 MPa in Fig. 12 for the microvoids pattern, while the maximum values of M_C with respect to 9 voids is 242 N under the critical loading 402 MPa. The same feature can be found for the microcracks pattern in Fig. 13. The present characteristic agrees with the intuitional understanding that more cracks or voids weaken the integrity and strength of multi-damaged materials and yields a higher damage level. The most important feature of M_C is that they are essentially different for various defect configurations. They are found to be greatly affected by defect pattern and density. It denotes that the critical values of the M-integral at final failure are configuration-dependent and there is no correspondence between the critical values of the M-integral and the specific configuration.

3.4 The proposed failure criterion as configurational damage parameter

It is well known that the J-integral is widely used as energy fracture parameters to predict the single-cracked problem, that is $J\,J_C$ where J-integral is evaluated as the energy release rate associated with crack extension and J_C is experimentally measured as the material-specific strength. However, the J-integral by itself is limited due to its local energy associated with the single distinguished crack. In many engineering structures, the overall strength is substantially degraded by evolution and propagation of a system of distributed defects rather a single continuous crack. The global characteristic of the M-integral calculated along the contour enclosing the overall defects might be proposed as a potential parameter describing the global failure state of the multi-defect system. The use of M-integral as a parameter in describing the global failure is therefore of practical important. Similar as the application of the J-integral, a straightforward definition of failure criterion via the concept of M-integral can be proposed as

$$M \geq M_C, \tag{6}$$

where M-integral is evaluated as the global energy release rates associated with multi-defects self-similar extension and M_C is essentially the critical value of the M-integral at failure of materials. The efficient application of the M-integral as a failure criterion requires the premise that it should be experimentally measured as the problem-invariant constants regardless the configurations and sizes of multi-defects. However, numerical analysis in the present series of examples shows that the critical values of the M-integral at failure are definitely configuration-dependent. The global M-integral without any special treat is obviously not feasible for such an analysis due to the configuration-dependent property of M_C. In other words, the complete failure mechanism of the multi-damaged materials cannot be governed by a single parameter M_C. Rather, a configuration independent failure parameter should be introduced, and the proposed failure criterion should be only determined by the material intrinsic properties regardless the detailed defects just as the K_C or J_C in fracture mechanics.

According to the explicit analysis in Eq.(5), it is consistently assume that the M-integral can be expressed as

$$M = \Pi \sigma^2 A_D, \tag{7}$$

where A_D denotes the damaged area and consists two parts in the present analysis. One is the defect areas and the other the areas of plastic zone. The plastic zone is regards as one kind of 'damages'. In the numerical calculation, A_D is the whole area of the damaged zone localized at the center of the elastic specimen (as shown in Fig. 3).

The innovative idea is that the coefficient   termed as configurational damage parameter (abbreviated as -parameter) would play a significant role in evaluating the multi-damage medium. It should be always positive due to the positive energy release for the self-similar expansion of multi-defects. The newly proposed -parameter can be referred as a damage driving forces which is an unknown outside variable determined by the material behaviors, the configuration and size of multi-defects, the specific geometry of specimen et al. The innovative -parameter as anticipated will play a remarkable role to predict the damage evolution in the elastic-plastic material.

The most intriguing proposal of the present study is to introduce a failure criteria based on the -parameter as

$$\Pi \geq \Pi_C, \tag{8}$$

where   is defined by $M/(\ ^2A_D)$ and represents the damage level of the multi-defect system; $_C$ is the critical value of the -parameter at failure.

The special treatment and introduction of the failure theory vial the -parameter need be clarified and addressed. The most important issue arises whether $_C$ is a material-specific constant which is only determined by the material itself and regardless the circumstance of multi-defects. In order to address the question, Tables 2 and 3 show the critical value of -parameter calculated by $M_C/(\sigma_C^2 A_D)$ according to Eq.(7). Table 2 shows the critical values of the -parameter for various numbers of microvoids. The average of overall values is 1.018 10^{-11} Pa^{-1}, and the deviation is less than 0.5%. And Table 3 shows the critical -parameter for various numbers of microcracks. The average of overall values is 1.018 10^{-11} Pa^{-1}, and the deviation is less than 0.45%. Hence, we note that the invariant values of $_C$ approximately approach a constant of 1.018 10^{-11} Pa^{-1} for all cases of different multi-defect systems. It is intriguing to find that the critical -parameter appears to be invariant with respect to different defect configurations under the uni-axial tensile load. The present numerical results from various defect configurations support that $_C$ is just a material-specific constant which is determined by the strength of material itself regardless of the detailed defect configurations. It means that, the damage caused by different configuration of defects could be unified and described by the -parameter for its stiffness. The parameter could give the damage estimation of the defect zone for engineering application, which can be defined as a failure criterion to predict the evolution and degradation of such multi-defect failure condition ranging from the present of a finite number of microcracks and/or voids to the formation of densely and locally distributed microdefects with arbitrary configurations and sizes.

For practical purpose, the pragmatic approach to design for strength via the -parameter can follow the procedure as

i) Calculate the physical fields by solving the boundary-value problem in the multi-defected system. Calculate the -parameter by $M/(\ ^{2}A_D)$ where M is numerically integrated along the contour enclosing all defects in the local damage region, and A_D is evaluated by the areas of damaged zone.

ii) Measure the critical values of -parameter i.e., $_C$ using a simple sample of the material such as a tensile specimen. The critical values of -parameter can be calculated by the critical M-integral, the tensile load, and the corresponding damaged area at failure.

iii) Make sure that the maximum $_{max}$ in the body is below the strength of the material $_C$.

Furthermore, the critical values of the -parameter are determined at failure relying that the reduction of effective elastic moduli reaches a critical value. It means that the proposed failure theory via the concept of the M-integral can be the alternative and effective way to replace the reduction of effective elastic moduli, which has been widely adopted in damage mechanics. Furthermore, it is widely accepted that the calculation of effective elastic moduli greatly depends on the representative volume. For the realistic case of locally damage problem, it is generally believed that the multiple defects are heterogeneously and locally distributued in a region. It would be challenging to choose the appropriate representative volume to evaluate the reduction of effective elastic moduli. Fortunately, the application of the -parameter will overlap this issue. The intriguing feature of the proposed theory is that the -parameter can be calculated along the contour which encloses the multiple defects concerned in engineering. Based on the path-independent property of the M-integral, the values of the -parameter will be independent to the area enclosed by the contour. Thus the feature that the -parameter can be carried out in the arbitrary remote elastic region makes it more applicable in describing the associated material damage characteristic than the reduction of effective elastic moduli does. The present studies demonstrated that the -parameter could be used as a new failure criterion to describe the damage behavior of a multi-defect mechanical system similar as what the *J*-integral does in fracture mechanics.

3.5 A protocol to experimentally measure the -parameter

The usefulness of the newly proposed -parameter relies on an effective and convenient experimental tool to measure it. The key technique to experimentally measure the -parameter is the evaluation of the *M*-integral in a damaged material. Previously, King and Herrmann (1981) proposed a nondestructive evaluation of the *M*-integral for the special simple crack cases with the proper choice of the contour *C*, and it requires only a single specimen of fixed crack length. Zuo and Feng (2012) improved the nondestructive technique by modifying the approximate formulas to calculate the *M*-integral and select the appropriate the integral contours. They make use of many strain gages to measure the displacements and strains at specific points on the specimen and determine the *M*-integral by the approximate, semi-explicit expression through the measured displacements. However, their techniques are limited by certain special specimen geometries in linear elasticity, certain simplifying assumption regarding the terms in the integrand (as was only true for the centre-cracked and edge-cracked panel).

Recently, there are a few of researches concerned to experimental studies and measurements of the *M*-integral by the modern optic instruments. The present authors proposed a technique by using digital image correlation for evaluating the *M*-integral. The corresponding experimental procedure can refer to the reference by Yu et al. (2012). The experimental arrangement is depicted in Fig. 14(a). The specimens with changing gray values as they occur with random pattern are more appropriate. Therefore, the specimens are pretreated with powder sprays to obtain the high contrast stochastic pattern (See Fig. 14b). The method makes direct use of the definition of *M*-integral as a contour integral and involves experimental evaluation of the integrand at various points along an arbitrary contour and then determinates the *M*-integral by numerical integration. Determination of the integrand of *M*–integral involves knowledge of all the components in the x_1-x_2 plane including the strain energy density, the strains, the stresses, and the displacement gradient tensors. A smooth method is proposed to evaluate and calibrate the measured displacements which are used to calculate strains and the differentials of the displacements with respect to the axes at various points along the integration contour. Meanwhile, the Ramberg-Osgood nonlinear elastic-plastic theory (Ramberg and Osgood, 1943) is employed to determine the stresses. The total strain energy density is calculated by numerical integration of the evaluated nonlinear stress-strain curves for the material. Experimental values of the *M*-integral are found to agree well with the corresponding numerical analysis. Therefore, this appears to be a viable technique for non-destructive experimental evaluation of the *M*-integral in the locally distributed multi-damaged materials. The material strength for the -parameter can be obtained by the derivation of the critical values of the *M*-integral, the critical tensile loading, and the damaged area including the defects area itself and the plastic area. The plastic zone can be evaluated by the strain beyond the residual yielding strain. The failure phenomenon of the multi-defects could be the growth of the microcracks, the coalescence of microvoids, the nucleation of microcracks and so on. They can be instantaneously reported by the high rate photographic instrument to determine the failure initiation.

4. Conclusions and remarks

After performing the above analysis, we summarize the following conclusions:

1) There apparently exist the physical explanations of the configurational forces associated with the *M*-integral, which can be interpreted as the global energy release rate due to self-similar expansion of multiple defects provided that the integral contour encloses all the microdefects. Besides this, the contribution induced by the formation of overall microdefects in the solids to the J_k-integral vanishes, and the *L*-integral generated by the rotation of the microdefects are negligible compared with the remarkable values of the *M*-integral. The present findings of the invariant integrals regarding the J_k-, *M*-, and *L*-integral demonstrate that only the *M*-integral play an important role in description of multi-damaged solids. It can provide an effective measure for evaluating the damage level.
2) Numerical results of the *M*-integral for some series of variable examples with different defect patterns and density reveal that the critical value of the *M*-integral characterized by M_C is not a problem-invariant constant. M_C shows an apparent

configuration-dependence. The failure evolution cannot be governed by the theory of M M_C. An innovative failure theory via the concept of *M*-integral is proposed by introduction of a new failure -parameter which critical value is only determined by the material-specific behavior regardless of the detailed defect configurations.

3) The inherent relation between the *M*-integral and the reduction of effective elastic moduli exists by the present numerical and theoretical analysis. The present useful findings can lead us to propose a new failure parameter as the -parameter, which is defined via the concept of the *M*-integral, the remote load, and the damaged area. In contrast with the straight application of the *M*-integral as a failure parameter, the present formulation of the -parameter can guarantee a constant material-specific strength whatever the damage levels are. A convenient framework of the proposed failure theory via the -parameter is suggested to the engineers to predict the failure of multiple defect system, just like the application of *K*-factor or *J*-dominant criterion in classic fracture mechanics.
4) A protocol technique achieved by method of digital image correlation provides an effective and convenient tool to evaluate the -parameter. It evaluates all physical quantities of the integrand of the *M*-integral at various points along the integral contour enclosing the defect zone and calculates the *M*-integral by numerical integration. And then the -parameter can be directly determined by the *M*-integral, the remote load, and the corresponding damaged area.
5) Potential applications of the newly proposed -parameter via the concept of configurational forces associated with the *M*-integral would be remarkable. The -parameter during the evolutionary microdefects just represents the progressive energy release rate due to the damage growth, e.g., microcracks growth, microvoids coalescence, and microcracks nucleation et al. The -parameter can provide an outside variable features in description of microdefects damage evolution. Particularly, it has advantage of predicting the failure of material with the locally distributed multi-defects to overlap the shortcoming of classic failure theory. In such special case, the local fracture parameters, such as *K* and *J,* are hard to calculate since there is no a single, major, continuous crack. The classic damage mechanic via the effective elastic moduli is either constricted since it

would be inaccurately determined due to the sensitivity to the area without continuously distributed defects.

Acknowledgement

This work was supported by the National Natural Science Foundation of China with grant No. 11202156, No. 10932007 and No.11021202 and the Fundamental Research Funds for the Central Universities in China.

Appendix A: The contribution of the nonlinear elastic energy to the *M*-integral for the defect-free medium

Here, we introduce the third path denoted by - C_s, which bypasses the defect zones and only encloses the homogeneity, as shown in Fig. 2(c). Thus, the *M*-integral over path is defined by:

$$M^{\Omega} = M^{\Gamma} - \sum M^{(s)} = \oint_{\Omega} \left(W x_i n_i - T_k u_{k,i} x_i \right) ds. \tag{A.9}$$

By using Green's theorem, the first term $\oint_{\Omega} W x_i n_i ds$ in Eq.(A.9) can be written as

$$\oint_{\Omega} W x_i n_i ds = \oint_{\Omega} W x_1 dx_2 - \oint_{\Omega} W x_2 dx_1 = \iint_{A(\Omega)} 2W dx_1 dx_2 + \iint_{A(\Omega)} (\frac{\partial W}{\partial x_1} x_1 + \frac{\partial W}{\partial x_2} x_2) dx_1 dx_2, \tag{A.10}$$

where A( ) means the area which is surrounded by the closed path .

Making use of the stress equilibrium with the absence of body force, the term $\frac{\partial W}{\partial x_1} x_1$ is formulated as

$$\frac{\partial W}{\partial x_1} x_1 = \frac{\partial W}{\partial \varepsilon_{ij}} \frac{\partial \varepsilon_{ij}}{\partial x_1} x_1 = \sigma_{ij} \frac{\partial \varepsilon_{ij}}{\partial x_1} x_1 = \sigma_{ij} \frac{\partial}{\partial x_1} (\frac{\partial u_i}{\partial x_j}) x_1 = \frac{\partial}{\partial x_j} (\sigma_{ij} \frac{\partial u_i}{\partial x_1}) x_1. \tag{A.11}$$

Similarly,

$$\frac{\partial W}{\partial x_2} x_2 = \frac{\partial}{\partial x_j} (\sigma_{ij} \frac{\partial u_i}{\partial x_2}) x_2. \tag{A.12}$$

From Eq.(A.11) and(A.12), Eq.(A.10) can reduce to be

$$\oint_{\Omega} W x_i n_i ds = \iint_{A(\Omega)} \left[2W + \frac{\partial}{\partial x_j} (\sigma_{ij} \frac{\partial u_i}{\partial x_k}) x_k \right] dx_1 dx_2. \tag{A.13}$$

Meanwhile, the second term $\oint_{C} T_k u_{k,i} x_i ds$ in Eq.(A.9) can be written as:

$$\begin{aligned}\oint_{\Omega} T_k u_{k,i} x_i ds &= \oint_{\Omega} \sigma_{k1} u_{k,i} x_i dx_2 - \oint_{\Omega} \sigma_{k2} u_{k,i} x_i dx_1 \\ &= \iint_{A(\Omega)} \left(\frac{\partial(\sigma_{kj} u_{k,i})}{\partial x_j} x_i + \sigma_{kj} u_{k,i} \frac{\partial x_i}{\partial x_j}\right) dx_1 dx_2 \qquad \text{(A.14)} \\ &= \iint_{A(\Omega)} \left[\sigma_{ij} u_{i,j} + \frac{\partial}{\partial x_j}\left(\sigma_{ij} \frac{\partial u_i}{\partial x_k}\right) x_k\right] dx_1 dx_2 .\end{aligned}$$

Substituting Eq.(A.13) and Eq.(A.14) into Eq.(A.9), the *M*-integral integrated along the path can be formulated as

$$M^{\Omega} = M^{\Gamma} - \sum M^{(s)} = \iint_{A(\Omega)} (2W - \sigma_{ij} u_{i,j}) dx_1 dx_2 . \qquad \text{(A.15)}$$

For a nonlinear elastic state, the strain energy density W is assumed to be a homogeneous function of strain and can be expressed as (Chen and Shield, 1977)

$$W = \frac{1}{N} \sigma_{ij} u_{i,j} \qquad \text{(A.16)}$$

with N being an integer. Substituting Eq.(A.16) into Eq.(A.15), one obtain

$$M^{\Omega} = M^{\Gamma} - \sum M^{(s)} = \frac{2-N}{N} \iint_{A(\Omega)} \sigma_{ij} u_{i,j} dx_1 dx_2 . \qquad \text{(A.17)}$$

For the defect-free material in which there is no defect inside the body, $\sum M^{(s)}$ will be vanished. And then the value of *M*-integral can be finally reduced as

$$M^{\Gamma} = \frac{2-N}{N} \iint_{A(\Omega)} \sigma_{ij} u_{i,j} dx_1 dx_2 . \qquad \text{(A.18)}$$

N=2 for linear elastic material, therefore, the *M*-integral is zero in the linear traction-free elasticity. Nevertheless, N 2 for the nonlinear elastic material. It can conclude that the nonlinear elastic energy enclosed by the integral contours will have a significant contribution on the values of the *M*-integral.

Appendix B: The *M*-integral for an infinite elastic matrix containing a circular inhomogeneity

The analytical solutions to the stress-strain fields in plane elasticity can be referred to the complex variable function method (Muskhelishvili, 1953). The stresses ($_{xx}$, $_{yy}$, $_{xy}$) and the displacements (u_x, u_y) in an infinite elasticity can be expressed in terms of two complex potentials (z) and (z)

$$\begin{aligned}&\sigma_{xx} + \sigma_{yy} = 4\,\mathrm{Re}[\varphi'(z)], \\ &\sigma_{yy} - \sigma_{xx} + 2i\sigma_{xy} = 2[\bar{z}\varphi''(z) + \psi'(z)], \qquad \text{(B.1)} \\ &2\mu(u_x + iu_y) = \kappa\varphi(z) - z\overline{\varphi'(z)} - \overline{\psi(z)},\end{aligned}$$

where μ=E/(2+2ν) is the shear modulus of elasticity, κ=(3-ν)/(1+ν) for the plane stress problem and κ=3-4ν for the plane strain problem.

Consider an infinite elastic matrix embedded with a circular inhomogeneity, the complex potentials of the elastic matrix can be written as

$$\begin{aligned}\varphi(z) &= \frac{\sigma}{4}\left(z+\frac{\beta R^2}{z}\right),\\ \psi(z) &= -\frac{\sigma}{2}\left(z+\frac{\gamma R^2}{z}-\frac{\delta R^4}{z^3}\right),\end{aligned} \tag{B.2}$$

where represents the remote uni-axial loading; R is the radius of the circular inhomogeneity; , , and are the material constants defined by

$$\beta = -\frac{2(\mu_0-\mu)}{\mu+\mu_0\kappa},\quad \gamma = \frac{\mu(\kappa_0-1)-\mu_0(\kappa-1)}{2\mu_0+\mu(\kappa_0-1)} \quad \text{and} \quad \delta = \frac{\mu_0-\mu}{\mu+\mu_0\kappa}. \tag{B.3}$$

where the subscript prima $\{\}_0$ refers to the material constants corresponding to the inhomogeneity.

Alternatively, the definition of the M-integral could be expressed in terms of the complex potentials,

$$M = \frac{4(1-\nu^2)}{E}\,\mathrm{Im}\oint_C z\varphi'(z)\psi'(z)dz. \tag{B.4}$$

Substituting Eq.(B.3) into Eq.(B.4) and integrating along the remote circular path, one can obtain

$$M = \frac{\pi\sigma^2 R^2}{E}(\gamma+\beta)(1-\nu^2). \tag{B.5}$$

Assume that the inhomogeneity has the reduction of Young's moduli E_0=(1-α)E, the parameters and can be written from Eq.(B.3)

$$\beta = -2\frac{E_0+E_0\nu-E-E\nu_0}{E+E\nu_0+3E_0-E_0\nu};\qquad \gamma = \frac{E-E\nu_0-E_0+E_0\nu}{E_0+E_0\nu+E-E\nu_0}. \tag{B.6}$$

Substituting Eq.(B.6) into Eq.(B.5), we finally obtain the expression of the M-integral for an infinite elasticity containing the circular inhomogeneity, that is

$$M = \frac{\pi\sigma^2 R^2(1-\nu^2)}{E}\left[\frac{(-3\nu^2-5)\alpha^2+(6\nu^2-6\nu\nu_0+8)\alpha+(-3\nu^2-3\nu_0^2+6\nu\nu_0)}{(-\nu^2+2\nu+3)\alpha^2+(2\nu^2-2\nu\nu_0+2\nu_0-4\nu-10)\alpha+(-\nu^2+2\nu\nu_0+2\nu-\nu_0^2-2\nu_0+8)}\right]. \tag{B.7}$$

References

Banerjee, B., Adams, D.O., 2004. On predicting the effective elastic properties of polymer bonded explosives using the recursive cell method. Int. J. Solids and Struct. 41,481-509.

Budiansky, B., Rice, J.R., 1973. Conservation laws and energy release rates. J. Appl. Mech. 40, 201-203.

Carka, D., Landis, C.M., 2011. On the path-dependence of the *J*-Integral near a stationary crack in an elastic-plastic material. J. Appl. Mech. 78, 011006.

Chang, J.H., Chien, A.J., 2002. Evaluation of *M*-integral for anisotropic elastic media with multiple defects. Int. J. Fracture 114, 267-289.

Chang, J.H., Peng, D.J., 2004. Use of *M* integral for rubbery material problems containing multiple defects. J. Eng. Mech. 130, 589-598.

Chang, J.H., Wu, W.H., 2011. Using *M*-integral for multi-cracked problems subjected to nonconservative and nonuniform crack surface tractions. Int. J. Solids Struct. 48, 2605–2613.

Chen, F.H.K., Shield, R.T., 1977. Conservation laws in elasticity of the *J*-integral type. J. Appl. Math. Phys. (ZAMP) 28, 1-21.

Chen, Y.H., 2001a. *M*-integral analysis for two-dimensional solids with strongly interacting cracks, Part I: In an Infinite Brittle Solids. Int. J. Solids and Struct. 38, 3193-3212.

Chen, Y.H., 2001b. *M*-integral analysis for two-dimensional solids with strongly interacting cracks, Part II: In the Brittle Phase of an Infinite Metal/Ceramic Biomaterial. Int. J. Solids and Struct. 38, 3213-3232.

Chen, Y.H., 2002. Advances in conservation laws and energy release rates. Kluwer Academic Publishers, Netherlands.

Chen, Y.H., Hasebe, N., 1998. A consistency check for strongly interacting multiple crack problems in isotropic, bimaterial and orthotropic bodies. Int. J. Fracture 89, 333-353.

Chen, Y.H., Lu, T.J., 2003. Recent developments and applications in invariant integrals. Appl. Mech. Rev. 56, 515-552.

Chen, Y.Z., 1986. A technique for evaluating the stress intensity factors by means of the *M*-integral. Eng. Fract. Mech. 23, 777–780.

Chen, Y.Z., 2003. Analysis of *L*-integral and theory of the derivative stress field in plane elasticity. Int. J. Solids and Struct. 40, 3589-3602.

Chen, Y.Z., Lee, K.Y., 2004. Analysis of the *M*-integral in plane elasticity. J. Appl. Mech. 71, 572-574.

Cherepanov, G.P., 1967. The propagation of cracks in a continuous medium. J. Appl. Math. Mech. 31, 503-512.

Choi, N.Y., Earmme, Y.Y., 1992. Evaluation of stress intensity factors in circular arc-shaped interfacial crack using *L* integral. Mech. Mater. 14, 141-153.

Eischen, J.W., Herrmann, G., 1987. Energy release rates and related balance laws in linear elastic defect mechanics. J. Appl. Mech. 54, 388-392.

Eshelby, J.D., 1975. The elastic energy-momentum tensor. J. Elasticity **5**, 321-335.

Ford, H., 1963. Advanced Mechanics of Materials. Longmans, London.

Freund, B.L., 1978. Stress intensity factor calculations based on a conservation integral. Int. J. Solids Struct. 14, 241-250

Griffith, A.A., 1921. Philosophical transactions of the royal society of london. Series A, containing papers of a mathematical or physical character 221, 163-198.

Herrmann, G.A., Herrmann, G., 1981. On energy release rates for a plane cracks. J. Appl. Mech. 48, 525-528.

Hu, Y.F., Chen, Y.H., 2009a. *M*-integral description for a strip with two voids before and after coalescence. Acta Mechanica 204, 109-120.

Hu, Y.F., Chen, Y.H., 2009b. *M*-integral description for a strip with two microcracks before and after coalescence. J. Appl. Mech. 76, 061017.

Hu, Y.F., Li, Q., Shi, J.P., Chen, Y.H., 2012. Surface/interface effect and size/configuration dependence on the energy release in nanoporous membrane. J. Appl. Phys. 112, 034302.

Hui, T., Chen, Y.H., 2010. The *M*-integral analysis for a nano-inclusion in plane elastic materials under uni-axial or bi-axial loadings. J. Appl. Mech. 77, 021019.

Irwin, G.R., 1957. Analysis of stresses and strains near the end of a crack traversing a plate. J. Appl. Mech. 24,361-364.

Kachanov, L.M., 1986. Introduction to Continuum Damage Mechanics. Martinus Nijhoff Publishers, Dordrecht.

Kanninen, M.F., Popelar, C.H., 1985. Advanced Fracture Mechanics. Oxford University Press, New York.

Kienzler, R., Herrmann, G., 1997. On the properties of the Eshelby tensor. Acta Mechanica 125, 73-91.

King, R.B., Herrmann, G., 1981. Nondestructive evaluation of the *J* and *M* integrals. J. Appl. Mech. 48, 83-87.

Knowles, J.K., Stermberg, E., 1972. On a class of conservation laws in linearized and finite elastostatics. Arch. Rational Mech. Anal. 44, 187-211.

Kuang, J.H., Chen, Y.C., 1996. The values of *J*-Integral within the plastic zone. Eng. Fract. Mech. 55, 869–881.

Lee, Y., Im, S., 2003. On the computation of the near-tip stress intensities for three dimensional wedges via two-state *M*-integral. J. Mech. and Phys. Solids 51, 825-850.

Li, Q., Chen, Y.H., 2008. Surface effect and size dependence on the energy release due to a nanosized void expansion in plane elastic materials. J. Appl. Mech. 75, 061008.

Li, Q., Hu, Y.F., Chen, Y.H., 2012. On the Physical Interpretation of the *M*-integral in Nonlinear Elastic Defect Mechanics. Int. J. Damage Mech. DOI: 10.1177/1056789512456860.

McMeeking, R.M., 1977. Finite deformation analysis of crack-tip opening in elastic-plastic materials and implications for fracture. J. Mech. Phys. Solids 25, 357–381.

Muskhelishvili, N.I., 1953. Some basic problems of the mathematical theory of elasticity. Noordhoff , Leyden.

Ramberg, W., Osgood, W.R., 1943. Description of stress-strain curves by three parameters. Technical Note No. 902, National Advisory Committee for Aeronautics, Washington DC.

Rice, J.R., 1968. A path independent integral and the approximate analysis of strain concentration by notch and cracks. J. Appl. Mech. 35, 379-386.

Seed, G.M., 1997. The Boussinesq wedge and the J_k, L, and M integrals. Fatigue Fract. Eng. Mater. Struct. 20, 907–916.

Wang, F.W., Chen, Y.H., 2010. Fatigue damage driving force based on the *M*-integral concept. Procedia Engineering 2, 231-239.

Yu, N.Y., Li, Q., Chen, Y.H., 2012. Experimental evaluation of the *M*-integral in an elastic-plastic material containing multiple defects. J. Appl. Mech. 1,347.

Zuo, H., Feng, Y.H., 2012. A new method for *M*-Integral experimental evaluation. Int. J. Damage Mech. DOI: 10.1177/1056789512442428

List of Tables Captions

Table 1. The fundamental concepts of material configurational forces regarding the J_k-, M-, and L-integrals.

Table 2. The critical value of -parameter for variable numbers of microvoids.

Table 3. The critical value of -parameter for variable numbers of microcracks.

ACCEPTED MANUSCRIPT

List of Figures Captions

Fig.1.(a) The picture of locally damaged material; (b) The schematic of the integration contour enclosing all microdefects to calculate the invariant integrals in the locally damaged material.

Fig.2. Self-similar expansion of one infinitesimal x_1, x_2-plane element corresponding to the configurational forces associated with the M-integral (a) along x_1-direction; (b) along x_2-direction and (c) self-similar expansion for the specific s-th defect.

Fig.3. Detailed configuration for the elastic-plastic plate with the multiple microvoids or microcracks randomly distributed in the local damage zone.

Fig.4. The nonlinear strain-stress curve of the Aluminum alloy LY-12 under monotonically increasing tensile loading.

Fig.5. Schematic of multiple microvoids randomly distributed in the local damage zone (a) 9 voids; (b) 16 voids; (c) 25 voids; (d) 36 voids; (e) 49 voids; (f) 64 voids; (g) 81 voids; (h) 100 voids; (i) 121 voids; (j) 144 voids; (k) 169 voids.

Fig.6. Schematic of multiple microcracks randomly distributed in the local damage zone (a) 9 cracks; (b) 16 cracks; (c) 25 cracks; (d) 36 cracks; (e) 49 cracks; (f) 64 cracks; (g) 81 cracks; (h) 100 cracks; (i) 121 cracks; (j) 144 cracks; (k) 169 cracks.

Fig.7. The calculated values of the M-integral against the external load for variable microvoids damage patterns.

Fig.8. The calculated values of the M-integral against the external load for variable microcracks damage patterns.

Fig.9. The calculated values of the effective elastic moduli against the external load for variable microvoids damage patterns.

Fig.10. The calculated values of the effective elastic moduli against the external load for variable microcracks damage patterns.

Fig.11. The inherent relation between the M-integral and the reduction of effective elastic moduli for the infinite matrix containing a circular inhomogeneity by an explicit analysis. The inner figure denotes the schematic of an infinite plane containing a circular inhomogeneity.

Fig.12. The critical values of the M-integral and the L-integral corresponding to the critical external load at failure for variable microvoids patterns.

Fig.13. The critical values of the M-integral and the L-integral corresponding to the critical external load at failure for variable microcracks patterns.

Fig.14. (a) The protocol to experimentally measure the -parameter by method of digital image correlation in multi-defects materials. (b) Powder sprays on the surface of specimen to obtain the good high contrast stochastic pattern.

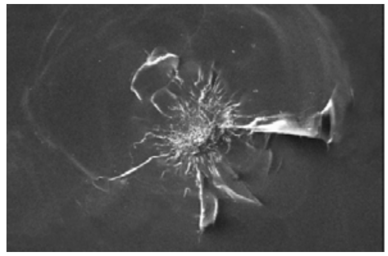

Fig. 1(a)

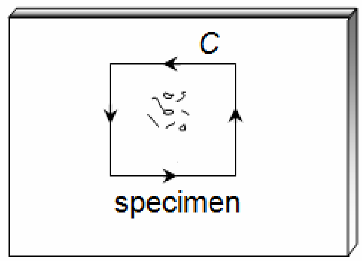

Fig. 1(b)

Fig. 1. (a) The picture of locally damaged material; (b) The schematic of the integration contour enclosing all microdefects to calculate the invariant integrals in the locally damaged material.

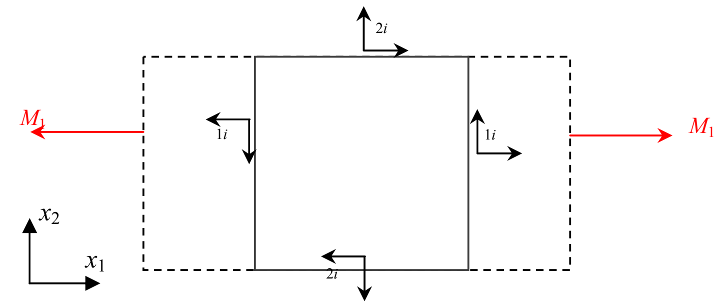

Fig. 2(a)

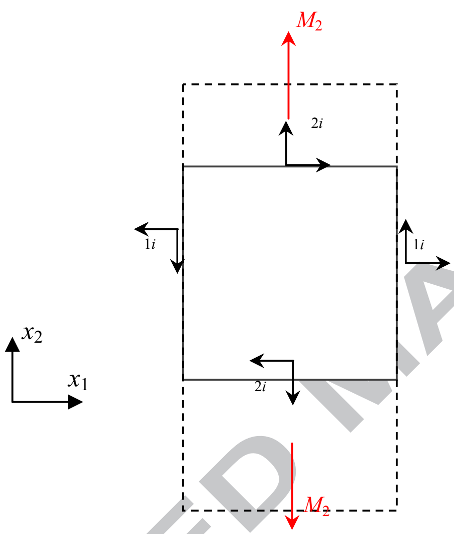

Fig. 2(b)

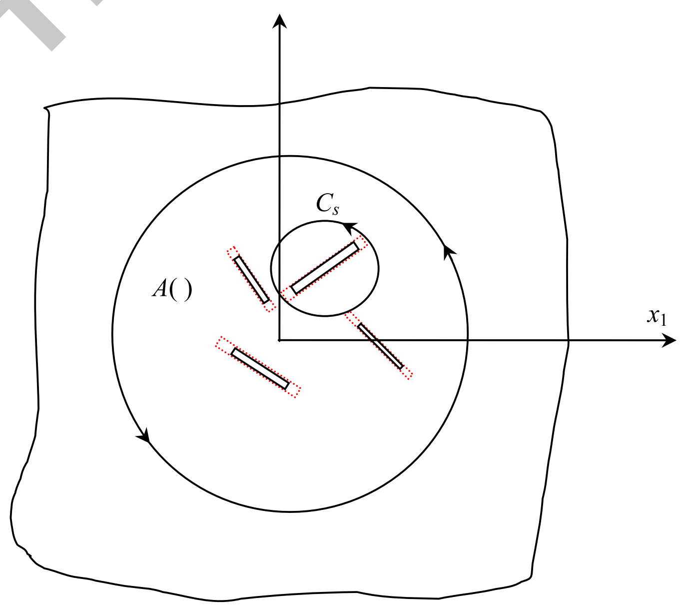

Fig. 2(c)

Fig.2. Self-similar expansion of one infinitesimal x_1, x_2-plane element corresponding to the configurational forces associated with the *M*-integral (a) along x_1-direction; (b) along x_2-direction and (c) self-similar expansion for the specific *s*-th defect.

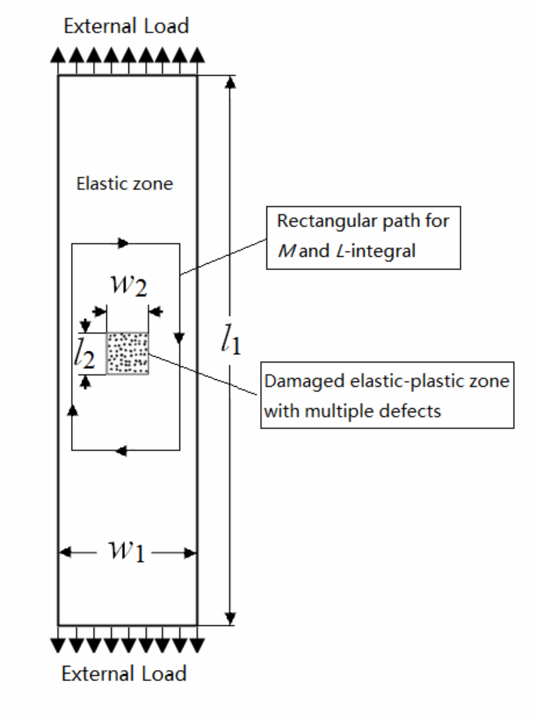

Fig. 3. Detailed configuration for the elastic-plastic plate with the multiple microvoids or microcracks randomly distributed in the local damage zone.

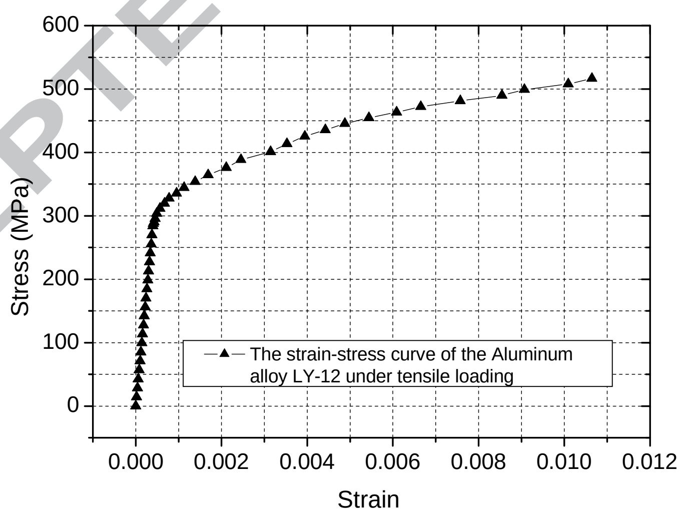

Fig. 4. The nonlinear strain-stress curve of the Aluminum alloy LY-12 under monotonically increasing tensile loading.

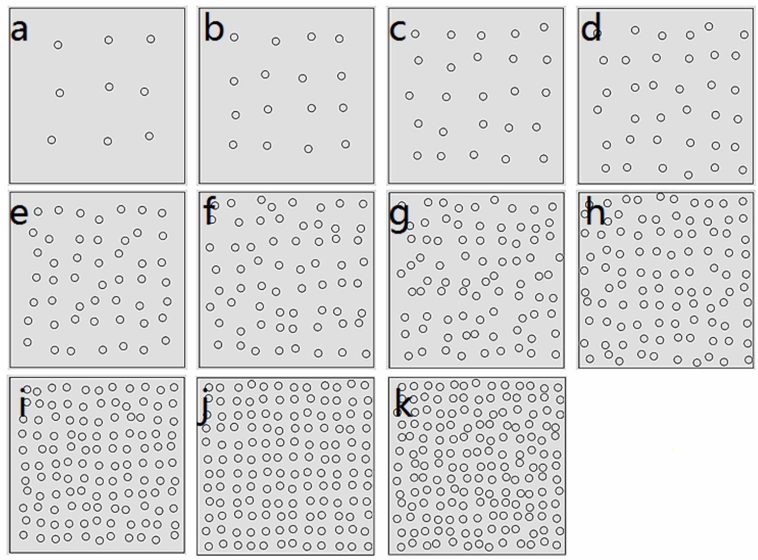

Fig. 5. Schematic of multiple microvoids randomly distributed in the local damage zone (a) 9 voids; (b) 16 voids; (c) 25 voids; (d) 36 voids; (e) 49 voids; (f) 64 voids; (g) 81 voids; (h) 100 voids; (i) 121 voids; (j) 144 voids; (k) 169 voids.

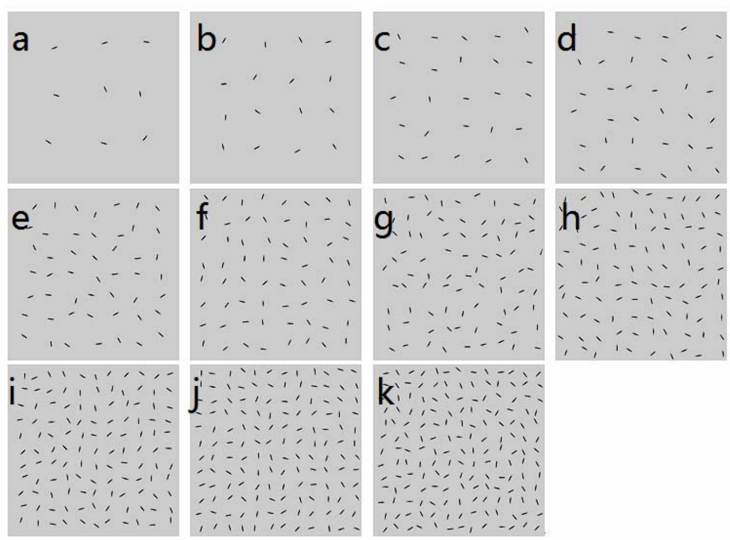

Fig. 6. Schematic of multiple microcracks randomly distributed in the local damage zone (a) 9 cracks; (b) 16 cracks; (c) 25 cracks; (d) 36 cracks; (e) 49 cracks; (f) 64 cracks; (g) 81 cracks; (h) 100 cracks; (i) 121 cracks; (j) 144 cracks; (k) 169 cracks.

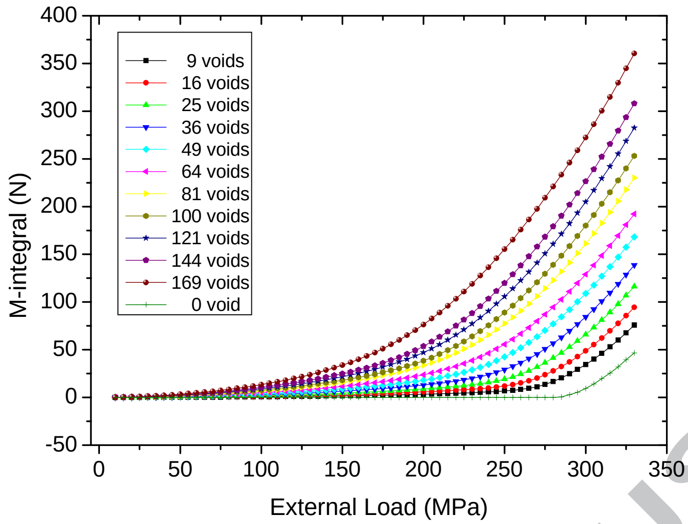

Fig. 7. The calculated values of the *M*-integral against the external load for variable microvoids damage patterns.

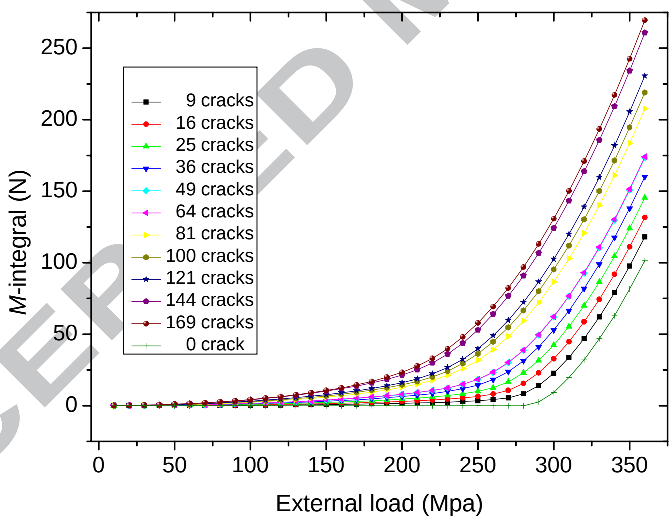

Fig. 8. The calculated values of the *M*-integral against the external load for variable microcracks damage patterns.

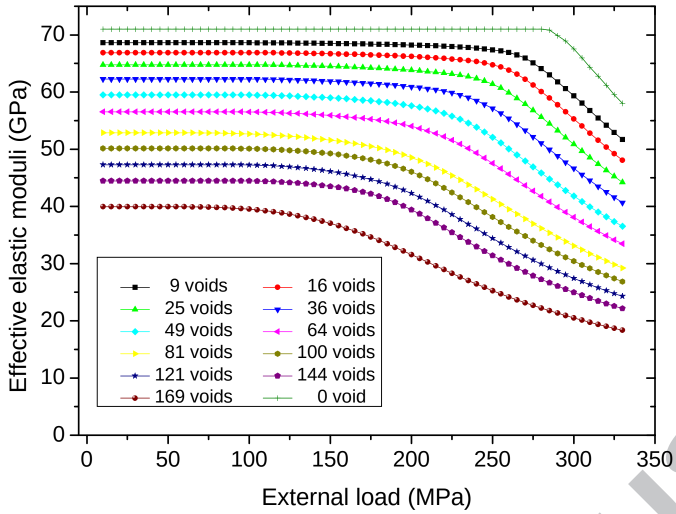

Fig. 9. The calculated values of the effective elastic moduli against the external load for variable microvoids damage patterns.

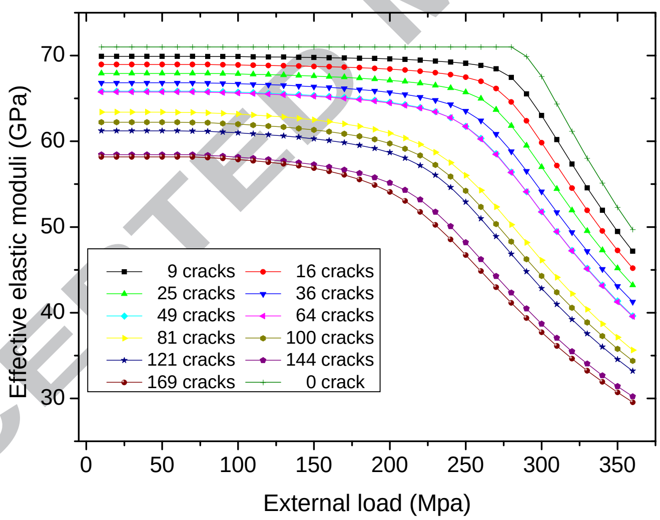

Fig. 10. The calculated values of the effective elastic moduli against the external load for variable microcracks damage patterns.

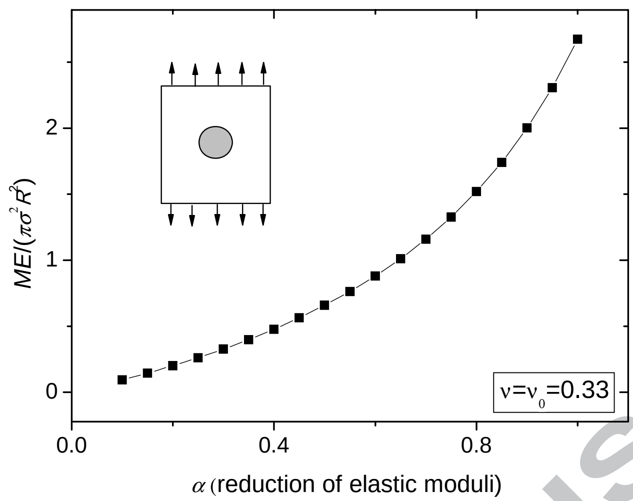

Fig. 11. The inherent relation between the *M*-integral and the reduction of effective elastic moduli for the infinite matrix containing a circular inhomogeneity by an explicit analysis. The inner figure denotes the schematic of an infinite plane containing a circular inhomogeneity.

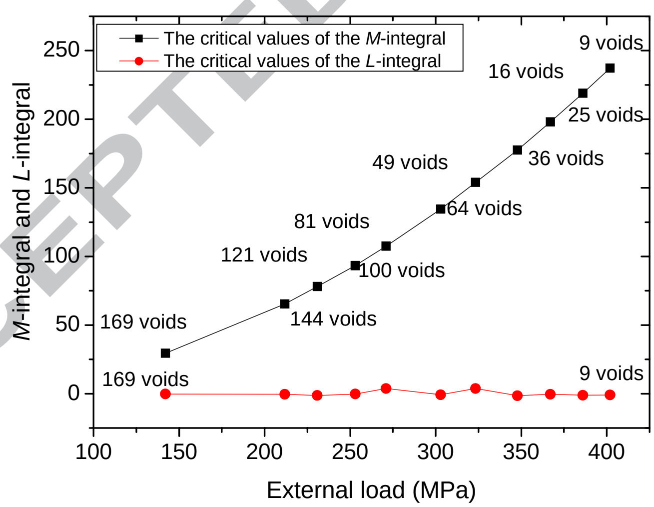

Fig. 12. The critical values of the *M*-integral and the *L*-integral corresponding to the critical external load at failure for variable microvoids patterns.

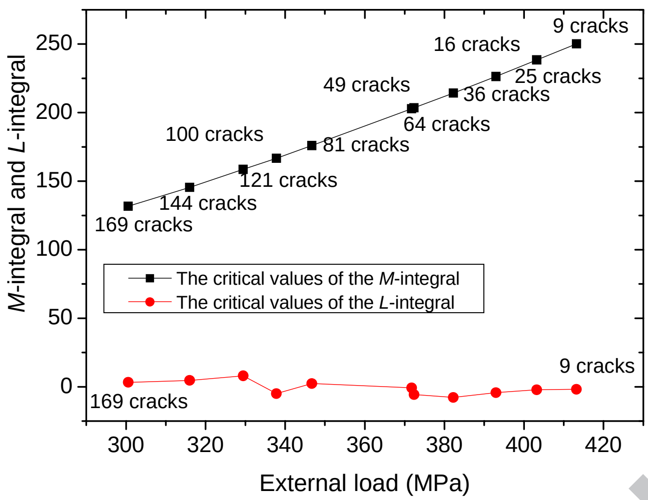

Fig. 13. The critical values of the *M*-integral and the *L*-integral corresponding to the critical external load at failure for variable microcracks patterns.

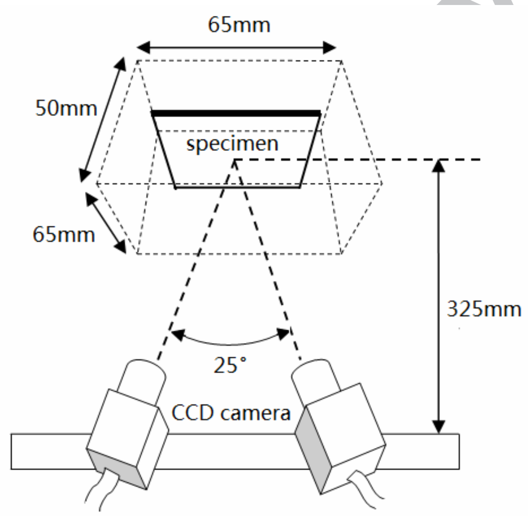

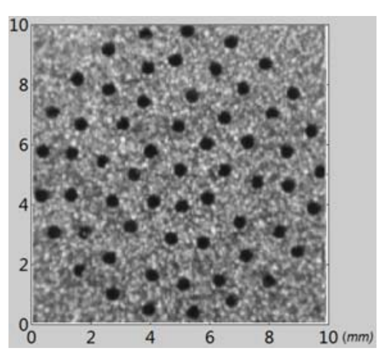

Fig. 14(a) Fig. 14(b)

Fig. 14. (a) The protocol to experimentally measure the -parameter by method of digital image correlation in multi-defects materials. (b) Powder sprays on the surface of specimen to obtain the good high contrast stochastic pattern.

Table 1. The fundamental concepts of material configurational forces regarding the J_k-, M-, and L-integrals

Operation	Definition	Configurational stress tensor	Damage sources	Equilibrium equation	Invariant integrals
Gradient	$\nabla(\Lambda) = -\left(\frac{\partial W}{\partial x_i}\right)_{\mathrm{expl}} - \sigma_{kj} u_{k,ji}$	$b_{ji} = W\delta_{ji} - \sigma_{jk} u_{k,i}$	$R_i = -\left(\frac{\partial W}{\partial x_i}\right)_{\mathrm{expl}}$	$b_{ji,j} + R_i = 0.$	$J = J_1 = \oint_C b_{j1} n_j ds = \oint_C (wn_1 - \sigma_{jk} u_{k,1} n_j) ds,$ $J_2 = \oint_C b_{j2} n_j ds = \oint_C (wn_2 - \sigma_{jk} u_{k,2} n_j) ds.$
Divergence	$\nabla \bullet (\Lambda \mathbf{x}) = -mW - \left(\frac{\partial W}{\partial x_i}\right)_{\mathrm{expl}} x_i$ $- \frac{\partial W}{\partial u_{k,j}} u_{k,ji} x_i$	$M_j = Wx_i\delta_{ij} - \sigma_{jk} u_{k,i} x_i + \frac{2-m}{2} \sigma_{ji} u$	$R = -\left(\frac{\partial W}{\partial x_i}\right)_{\mathrm{expl}} x_i$	$M_{j,j} + R = 0.$	$M = \oint_\Gamma \left(Wx_i n_i - \sigma_{jk} u_{k,i} x_i n_j + \frac{2-m}{2} \sigma_{ji} u_i n_j \right) d\Gamma.$
Curl	$\nabla \times (\Lambda \mathbf{x}) = -e_{mij} [(\frac{\partial W}{\partial x_i})_{\exp 1} x_j$ $+ \frac{\partial W}{\partial u_{k,l}} u_{k,li} x_j]$	$L_{ml} = e_{mij} (Wx_j \delta_{il} + \sigma_{il} u_j - \sigma_{kl} u_{k,i} x_j)$	$R_m = -e_{mij} [(\frac{\partial W}{\partial x_i})_{\exp 1} x_j$ $+ \left(\sigma_{ik} u_{j,k} - \sigma_{kj} u_{k,i} \right)]$	$L_{ml,l} + R_m = 0.$	$L = L_3 =$ $\oint_\Gamma e_{3ij} (Wx_j n_i + \sigma_{il} u_j n_l - \sigma_{kl} u_{k,i} x_j n_l) d\Gamma$

Nomenclature： σ_{kj} is the stress tensor; u_k denotes the components of displacements; W represents the strain energy density; n_i denotes the outside normal vector of the selected integral contour; the subscript prima$\{\}_{,i}$ refers to the corresponding differentiation with respect to the coordinate x_i; $\left(\partial W / \partial x_i\right)_{\mathrm{expl}}$ denotes the explicit dependence of W on x_i; m=$x_{i,i}$, which is identical to 3 for three dimensions and 2 for two dimensions; e_{mij} is the alternating tensor depending on the arrangement of the integer indices m, i, and j. e_{mij}=0 if any two of the indices are equal, e_{mij} =1 when the indices form an even permutation of (123), e_{mij}=−1 when the indices form an odd permutation of (123).

Table 2. The critical value of -parameter for variable numbers of microvoids

	Number of microvoids										
	9	16	25	36	49	64	81	100	121	144	169
$_{C}$ ($10^{-11}Pa^{-1}$)	1.019	1.020	1.020	1.019	1.022	1.018	1.017	1.014	1.018	1.017	1.015

Table 3. The critical value of -parameter for variable numbers of microcracks.

	Number of microcracks										
	9	16	25	36	49	64	81	100	121	144	169
$_{C}$ ($10^{-11}Pa^{-1}$)	1.017	1.018	1.018	1.017	1.019	1.019	1.017	1.017	1.015	1.012	1.014